

Study and Numerical Simulation of the Electrical Properties of a Duct-Type Electrostatic Precipitator Using Seven Circular Corona Wires: A Review

Angel Asipuela^{1*}, Tamás Iváncsy¹

¹ Department of Electric Power Engineering, Faculty of Electrical Engineering and Informatics, Budapest University of Technology and Economics, H-1521 Budapest, P.O.B. 91, Hungary

* Corresponding author, e-mail: asipuela.angel@vet.bme.hu

Received: 04 November 2021, Accepted: 14 June 2022, Published online: 04 July 2022

Abstract

The study of electrostatic precipitators (ESP) is of great importance in powder technology. Different physical and chemical processes occur during its operation. The objective of this investigation is to analyze and observe electrical phenomena using mathematical models such as Poisson's equation and the charge conservation equation. To carry out the simulation two flat plates and seven corona wires are geometrically arranged based on an ESP prototype. The general form of partial differential equations mentioned along with the boundary conditions was written in software and associated with the different parts of the geometry. For example, the electric field onset is calculated by Peak's law and set as one of the boundary conditions for the corona wires. Defining the space charge density distribution is an essential part because the next processes inside of ESP depend on this parameter. A specific method that splits the space charge density is used to solve these PDEs. Besides, a review of the concepts of the particle charging process, particle kinetics, and particle collection is introduced. The results obtained from the simulation such as the electric potential, electric field, and space charge density, agree with those proposed in some investigations.

Keywords

electrostatic precipitator, corona discharge, particle charging, Poisson's equation, charge density

1 Introduction

The study of electrostatic precipitators began many years ago. One of the first to generalize all the mathematical concepts and the start-up of these industrial types of equipment was White [1, 2]. Mathematical models have been proposed to analyze the charge of particles [1]; these models are generally complex expressions that describe the accumulation of charge on the particles subjected to an electric field and additional charges due to the interaction among them. In general, the shape of the particles is considered spherical, and the size of the particles is considered as the average of the sizes in different directions [1, 2]. Depending on the size of the particles, some models have been defined on interval functions in order to estimate how many particles of each type are collected or not [3, 4]. The properties of the particles are simplified in order to approach simple simulation in terms of computation, however, researches advise to manage mixtures with different electric properties and different concentration in order to approach more accurate results [5, 6].

Current research works are referred to as the guidelines set by White [1]. However, on the topic of particle charging, new models have been proposed such as Lawless' model [4]. When a model is proposed, it is demonstrated by experimentation, in the case of ESP's models, those have been tested and the analysis, relationships among the parameters have been obtained. For example, White's model showed a linear relation between charge particle and the square of particle radius [7].

The electrical phenomenon that describes the ESP operation could be properly explained by the theory of electrical discharges in gases. One of them is the negative corona discharge that is mainly used in this type of industrial application [1, 8]. Moreover, the corona has been studied with experiments and numerical models, and its formation when an electric potential is increased until reaching an electric field level a few magnitudes before reaching a spark over [1].

The physical model that describes the electrical phenomenon of a duct-type ESP is defined by differential

equations (PDEs), such as Poisson's equation [1], and the charge conservation equation [9–11]. A boundary condition to solve Poisson's equation is referred to as the corona onset field which is defined by Peek's equation.

When the ESP begins to operate, the particles in the gas volume start to be charged and are transported at a defined speed, and then they will pass to a stage where they will be collected by electrical attraction. The study of the particle kinetics also leads to an exhaustive analysis of the conditions in which the particles are moving [12]. Due to the molecular structure of gases, for example, the Cunningham correction factor [1], which is introduced to compensate for particle carryover especially when those are about 0.2 μ in radius.

When the particles have been charged, these will be electrically attracted to the collecting plates, this process is known as the study of particle collection. Also known as the collection-efficiency equation; which is defined by a probability theory study. This equation depends on the processes associated with an ESP, so it is related to the geometric arrangement, the drift velocity, the charged particle, and the gas flow [1]. For example, in some research works about ESP and its geometry, results have shown the relationship between the collection efficiency and the specific collection area [3]. New research works are being led to gas flow studies to improve the collection efficiency such as eddy reduction [13, 14]. Other cases have involved using practical mechanisms trying to improve the collection efficiency, for example, spreading water on the collecting plates for a defined period for removing the dust layer [15].

In Powder Technology, new studies are being conducted to create better models to describe the physical and chemical processes in ESP's. In addition, a few experiments have been performed to examine the Electrohydrodynamic (EHD) flow using various types of collecting plates. Mostly, numerical solutions proposed an overview about what will happen if some modifications are made in the physical structure [16–18]. Many topics can be studied in this field; however, in this initial stage of research, only the study of some electrical parameters in a specific ESP geometrical arrangement is carried out.

2 Physical model

To understand the operation of an ESP and the models that describe it, the following concepts are introduced.

2.1 Corona discharge

The free charges generated by the corona discharge phenomena have been considered one of the technically

feasible and economically competitive methods. It has been proved to be one of the best techniques for collecting and retention of particles in heavy industrial applications [1]. There are free charge carriers in the normal air due to ionizing radiation (background nuclear radiation and ultraviolet light radiation). Most gases are not perfect insulating materials; however, they are good for insulating purposes. The active zone that is generated is very small or considered a plasma with no net charge [1]. There are models for cold plasmas such as the corona discharge, however, this is not covered in this current paper [19].

2.2 Ionization process

Electron-impact ionization is the most common method for ionization, however, "*for the discharge for becoming self-maintaining a feedback mechanism is needed to supply the initiating electrons* [1]". There are two processes defined by plasma chemistry that help to understand the electrical discharge as shown in Eqs. (1) and (2). The first one is the ionization process specified as the gas-phase in volume reactions (homogeneous).



The second is the secondary emission process specified in the case of gas-surface reactions (heterogeneous):



e^- represents an electron, AB refers to molecules or compositions, and srf is the collision surface.

Townsend's investigation defined the chain reaction, where each new electron produced generates new electrons by ionization. That chain reaction is modeled mathematically as [1]:

$$dn = \alpha_r ndr, \quad (3)$$

where dn is the incremental increase in the number of electrons produced by n electrons moving a distance dr in the field, α_r is a coefficient that depends on gas and is a function of the field strength and gas pressure (gas density) [1]. It can be expressed in terms of electron currents per unit time:

$$i = i_0 e^{\alpha_r r}. \quad (4)$$

The positive ions produced by the first ionization process cause the secondary emission process, a continuous and repetitive process explains the chain reaction, and it can be described by Eq. (5):

$$i = i_0 e^{\alpha_r r} / 1 - \gamma (e^{\alpha_r r} - 1). \quad (5)$$

2.3 Electrical model

The corona discharge can be defined by Poisson's equation as shown in Eq. (6) [1]:

$$\nabla^2 \phi = -\frac{\rho}{\epsilon_0}, \quad (6)$$

$$\mathbf{E} = -\nabla \phi, \quad (7)$$

$$\mathbf{J} = \rho(\mathbf{KE} + \mathbf{u}) - D\nabla \rho, \quad (8)$$

and the charge conservation equation which describes the local accumulation and motion of charge as shown in Eqs. (8) and (9) [9]:

$$\frac{\partial \rho}{\partial t} + \nabla \cdot \mathbf{J} = 0. \quad (9)$$

ϕ (V) electric potential, ρ (C·m⁻³) space-charge density, ϵ_0 is the free-space permittivity 8.854×10^{-12} (F·m⁻¹), \mathbf{E} (V·m⁻¹) the electric field intensity, \mathbf{J} (A·m⁻²) the current density, K (m²·V⁻¹·s⁻¹) the ion mobility or mobility of charge carriers [9], \mathbf{u} (m·s⁻¹) the velocity of gas flow, and D (m²·s⁻¹) the diffusion coefficient of ions.

In general, the drift velocity is much higher than the velocity of the gas flow and the space-charge density is uniform with time, therefore, the Eqs. (8) and (9) can be expressed as follows:

$$\nabla(\rho \mathbf{KE} - D\nabla \rho) = 0, \quad (10)$$

2.4 Onset voltage and electric field

When the onset stage is reached, the plasma region bounded by r_0 near to the wire radius defines the onset electric field and potential E_0 and V_0 . These are calculated by the Eqs. (11) and (12). Nevertheless, r_0 cannot be exactly defined, but it can be estimated as a little more than the radius of the glow region [1, 9]:

$$E_0 = 30 \cdot f \cdot \delta \left(1 + 0.30 \sqrt{\delta / r_0}\right), \quad (11)$$

$$V_0 = r_0 E_0 \log \frac{d}{r_0}. \quad (12)$$

Due to the composition of the wire, a roughness factor was introduced ($f < 1$, in experimental laboratory 0.5–0.7) [1]. In general, Peek's equation is the reference for most research works. Depending on the corona wire E_0 is defined for a cylindrical and spherical (barbed electrode) geometry in Eqs. (13) and (14) [10].

Cylindrical geometry:

$$E_0 = 31\delta \left(1 + 0.308 / \sqrt{\delta r_0}\right). \quad (13)$$

Spherical geometry, a barbed electrode, i.e., a spheroidal tip.

$$E_0 = 31\delta \left(1 + 0.308 / \sqrt{0.5\delta r_0}\right) \quad (14)$$

$$\delta = \frac{T_0}{T} \cdot \frac{P}{P_0} \quad (15)$$

E_0 (kV·cm⁻¹) is the onset electric field, r_0 (cm) is the radius of corona wire, δ is a relation between the temperature and pressure, see Eq. (15), T_0 (293 °K), P_0 (760 mm Hg), and T and P are the operating values.

2.5 Particle charging

Two types of charging mechanisms are active in the field corona, the first charging process is due to the electric field, and the second is the diffusion charging process, particle charging occurs owing to phenomena of ion diffusion, in general terms, ions are transported by the electric field and Brownian motion (predominant in particles smaller than 0.2 μ [1, 20]) which depends on the thermal energy of the ions, rather than the electric field [1].

2.5.1 Field charging process

When an uncharged spherical particle of radius a is placed in a corona-discharge field, it will start to be charged, and the charging mechanism will depend on the flow of the gas ions [1]. Additionally, the particles further are also charged due to the continuous ion current from the corona electrodes to the collecting electrodes. Smith and McDonald defined a model for the particle charging calculations which is much more accurate than the one described by White [3] as shown in the Eqs. (16) and (17):

$$\frac{dq_f}{dt} = \frac{N_0 e K q_{fs}}{4\pi\epsilon_0} \left(1 - \frac{q_f}{q_{fs}}\right)^2, \quad (16)$$

$$q_{fs} = 4\pi\epsilon_0 E_0 (a + \chi)^2 \left[1 + 2 \frac{D-1}{D+2} \frac{a^3}{(a + \chi)^3}\right], \quad (17)$$

$$q_f = q_{fs} \frac{t}{t + t_0}, \quad (18)$$

where q_f (coulomb) is the charge obtained by the field, N_0 (ions·m⁻³) is the ions concentration, e (4.80×10^{-10} esu) is the electronic charge, K the ion-mobility, q_{fs} (coulomb) is the modified saturation charge, a (m) is the particle radius, C (m·s⁻¹) is the kinetic theory root-mean-square velocity of ions, D the dielectric constant, and χ is an adjustable parameter [3].

2.5.2 Diffusion charging process

The thermal motion causes the ions to diffuse through the gas, therefore some collisions among liquids or solids may occur. These ions will adhere to the particle by electrical-image forces. Ion diffusion provides a particle-charging mechanism that does not depend on an external agent as an electric field requires. The accumulated charge in the particle prevents it to attract other particles [1]. The equation which represents this process comes from White [1] as a reference of Arendt and Kallmann's research, the Eqs. (19) and (20) describes the particle charging by diffusion [1, 20].

$$\frac{dq_d}{dt} \left(1 + \frac{a^2 C}{4q_d K e} \right) = \pi a^2 C N_0 \exp\left(-\frac{q_d e^2}{akT}\right) \quad (19)$$

$$q_d = \frac{akT}{e^2} \ln\left(1 + \frac{\pi a C N_0 e^2 t}{kT}\right) \quad (20)$$

q_d is the charge by a diffusion process, a (cm) is the particle radius, k is the Boltzmann constant, T (°K) is the absolute temperature, and t (s) is the time [7].

2.6 Particle charging model by Lawless field-diffusion approach (dimensionless)

Lawless introduced an analytic charging rate model for upper and lower charging bounds for a continuous charging process. The analysis behind this model has followed a different path from the conventional field-diffusion approach [4]. Based on the symmetry between the charging rates for positive and negative charges of the same magnitude proposed by this model, the bipolar charging rate can be a modification of a unipolar charging rate [4]. The classical field charging rate is denoted in Eq. (21):

$$\frac{dv}{d\tau} = F(v, E_L) \equiv \begin{cases} \frac{3}{4} E_L \left(1 - \frac{v}{3E_L}\right)^2, & -3E_L \leq v \leq 3E_L \\ 0, & v > 3E_L \\ -v, & v < -3E_L \end{cases}, \quad (21)$$

where $v = qe^2/4\pi\epsilon akT$ is the self-potential of the particle, $E_L = aEe/kT$ is the electric field, $\tau = \beta \cdot u \cdot t/\epsilon$ is the time; β is the ion exposure time, u means the relative ion density, and t is the actual current time, $F(v, E_L)$ is called field charging rate, $3 E_L$ is called the saturation rate, $1/4$ comes from the choice of dimensionless time, and 3 represents the assumption of conductive particles and it is lower for

dielectrics [4]. The case of the classical continuum diffusion charging is expressed as follows in Eq. (22):

$$\frac{dv}{d\tau} = B_e(v) \equiv \frac{v}{\exp(v) - 1}, \quad (22)$$

where B_e is the Bernoulli function; for ($v = 0, B_e(0) = 1$). The case of unipolar charging model $M(v, E_L)$ is expressed by the Eqs. (23) and (24):

$$\frac{dv}{d\tau} = M(v, E_L) \equiv \begin{cases} F(v, E_L) + f(E_L) B_e(0), & -3E_L \leq v \leq 3E_L \\ f(E_L) B_e(v - 3E_L), & v > 3E_L \\ -v + f(E_L) B_e(-v - 3E_L), & v < -3E_L \end{cases}, \quad (23)$$

$$f(E_L) \equiv \begin{cases} \frac{1}{(E_L + 0.475)^{0.575}}, & E_L \geq 0.525 \\ 1, & E_L < 0.525 \end{cases}, \quad (24)$$

where $f(E_L)$ is an analytic fitting function. The charging rate of the particle at different locations can be calculated by [12]:

$$\frac{dq}{dt} = \frac{dv}{d\tau} \cdot \frac{4\pi akT \beta u}{e^2}. \quad (25)$$

2.7 Particle kinetics

In gas, the motion of suspended charged particles can be calculated by the laws of mechanics and electrical principles as is described by Eq. (26), since the particles are small the effects of gravity can be neglected [1]:

$$m \frac{dw}{dt} = qE_p - \frac{6\pi\eta a_p w}{C_c}, \quad (26)$$

where m is the mass, w is the drift velocity, q is the charge, a_p is the radius of the particle, E_p is the peek collection-field intensity, and η is the gas viscosity, and C_c is the Cunningham correction factor [1, 20]. Assuming the particle will reach a uniform velocity when is attracted, the velocity rate can be $dw/dt = 0$, as a result, Eq. (26) is expressed by Eq. (27):

$$w = \frac{E_p C_c}{6\pi\eta a_p} q = w = \frac{E_p C_c}{6\pi\eta a_p} (q_f + q_d). \quad (27)$$

With the sum of the field and diffusion charges the last equation, see Eq. (28) can be expressed [20, 21] in terms of a .

$$w(a_p) = E_p E_0 \alpha(a_p) \quad (28)$$

$$\alpha(a_p) = \frac{C_c}{6\eta} \left\{ \frac{4\epsilon_0 (a_p + \chi)^2}{a_p} \left[1 + 2 \frac{D-1}{D+2} \frac{a_p^3}{(a_p + \chi)^3} \right] + \frac{kT}{\pi e^2 E_0} \ln \left(1 + \frac{\pi C N_0 e^2 t}{kT} a_p \right) \right\} \quad (29)$$

The parameter $\alpha(a)$ is a correction coefficient, which relates the particle radius and charging behavior.

2.8 Particle collection

Charged, suspended particles are trapped by the electrical forces between the charges when they are close to the collecting electrodes. Relating the probability of particle capture in several sections with the physical construction of an ESP, Deutsch derived the collection efficiency [1], as shown in Eq. (30):

$$\eta = 1 - e^{-(A/Q) \cdot w(a_p)}, \quad (30)$$

where η is the grade efficiency of the particles collection, $A(\text{m}^2)$ is the collecting area, $Q(\text{m}^3 \cdot \text{s}^{-1})$ is the gas-flow rate and w the drift velocity.

In the case of a duct-type precipitator, the efficiency is expressed in terms of $L(\text{m})$ the precipitator length, $s(\text{m})$ the distance between the corona wire and one of the collecting plates, and v_g the gas velocity [1].

$$\eta = 1 - e^{-Lw(a_p)/sv_g} \quad (31)$$

3 ESP model and simulations

Different software programs have been used to investigate the phenomenon of particles traveling through an electric field and an ionized space. In this investigation, COMSOL Multiphysics is used to analyze the electrical properties in a duct-type ESP [11, 22–24].

3.1 ESP- Electrical modeling

3.1.1 ESP geometry

A prototype is available for the comparison of experimental and analytical data for future research [25]. The dimensions for the ESP geometry were taken from Fig. 1.

It would not be so practical to take all the ESP ducts for the simulation. In most research, one duct is enough for modeling, and the result of one can provide a clear idea of the whole system. Therefore, one duct is taken from this arrangement as shown in Fig. 2.

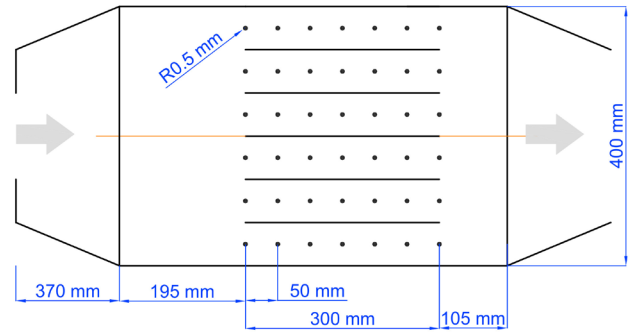


Fig. 1 ESP prototype geometrical arrangement and dimensions.



Fig. 2 Duct-type ESP arrangement.

3.1.2 Electrical model

In the stationary case, the corona discharge problem is solved under the conditions of two PDEs [11]: Poisson's Eq. (6) and charge conservation Eq. (10), neglecting the diffusion current the previous equations can be written as follows, see Eq. (32) [11]:

$$\nabla \phi \cdot \nabla \rho - \frac{\rho^2}{\epsilon_0} = 0. \quad (32)$$

To solve these PDEs, boundary conditions (BCs) must be defined [9, 12, 26]. In the case of the second-order equation for ϕ , it requires two BCs which are already as shown in Table 1. For the first-order equation of ρ needs only one BC, however, there is not a BC for ρ , at the emitter the charge density is unknown which brings complexity to find a solution for the PDEs [11]. One solution is approached splitting ρ in two parts:

$$\rho = \rho_\Omega + d\rho, \quad (33)$$

where ρ_Ω is constant in space, and $d\rho$ is space-dependent, assuming that ρ_Ω is known, the Eq. (13) can be written in terms of these parameters, as a result, the BC is defined as $d\rho = 0$ at the emitter electrode [27]. Moreover, at a

Table 1 Boundary conditions for the ESP arrangement.

PDE	BC	Element
$\nabla^2 \phi = -\frac{\rho}{\epsilon_0}$	$\phi = 0$	Collecting plates
	$\phi = U$	Corona wires
$\nabla \phi \cdot \nabla \rho - \frac{\rho^2}{\epsilon_0} = 0$	$n \cdot \nabla \phi = E_0$	Peek's formula

non-specific point P of the emitter, the boundary condition is defined as $0 = U - \phi$. Considering these definitions, the PDEs and boundary conditions were specified in the software. For example, in case of the Poisson's equation, one boundary condition is defined by Peek's equation, and computing this value gives $E_0 = 7.024 \cdot 10^3$ (kV/m). The electric potential used in this simulation is $U = -20$ (kV) for each corona wire.

3.1.3 Mesh

After understanding how to approach a solution, a triangular mesh is defined, see Fig. 3. The cell thickness is set up by a physics-controlled mesh, which provides a good representation of the results.

4 Results and discussion

The results of modeling the corona discharge [28, 29] are shown in Figs. 4(a) and (b), as White [1] illustrated the corona discharge, the potential curves, and the electric field are properly defined by Poisson's equation Eq. (6) and the Eq. (7).

Solving the PDEs for the space charge density [12, 30], the result of its distribution is shown in Fig. 5. To analyze

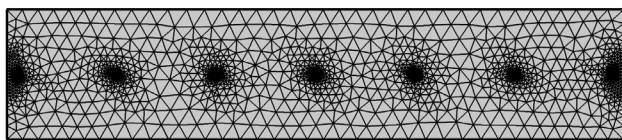


Fig. 3 Triangular mesh for 7 corona wires.

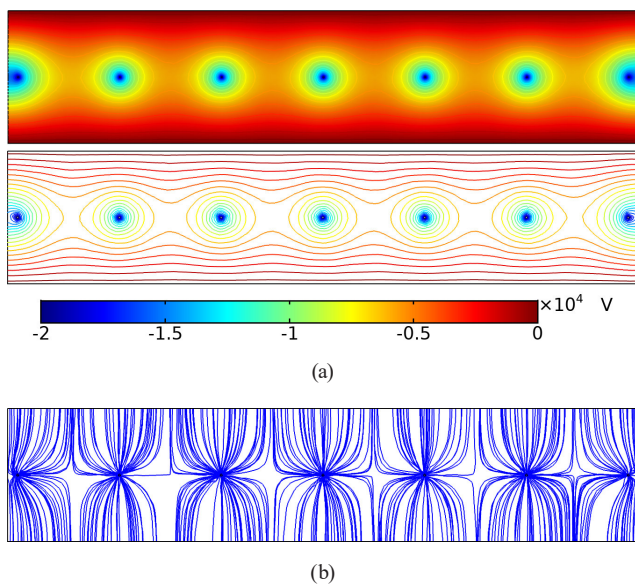


Fig. 4 The results of modeling the corona discharge; (a) Electric potential contour 0 to -20 [kV]; (b) Electric field.

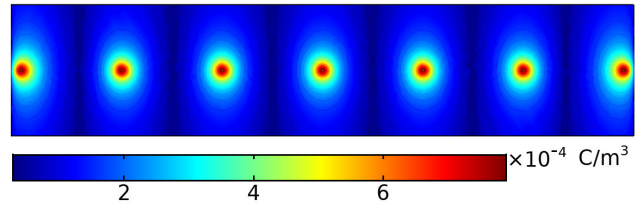


Fig. 5 Space charge density (C/m^3) distribution along the corona wires.

the magnitude of the electric potential [31], see Fig. 6, firstly, five cut lines were drawn at $y' = 0$ mm refers to the position $y = 32.5$ mm, meaning the cut line is crossing at the center of the corona wires, and the next cut lines are placed from the corona wires upwards to the collecting plate $y' = 0; 5; 10; 15; 20$ mm. For each cut line, the maximum potential value is located at the point concerning the axis of the corona wire, while the minimum potential value is defined at the half distance between the corona wires.

The same procedure is applied for the electric field, see in Fig. 7. The results of the maximum and minimum values are located similarly to the potential values previously described. However, the change in magnitude at each level is different from the behavior of the electrical potential.

In the second case, four perpendicular cut lines are drawn between the two collecting plates and the results are shown

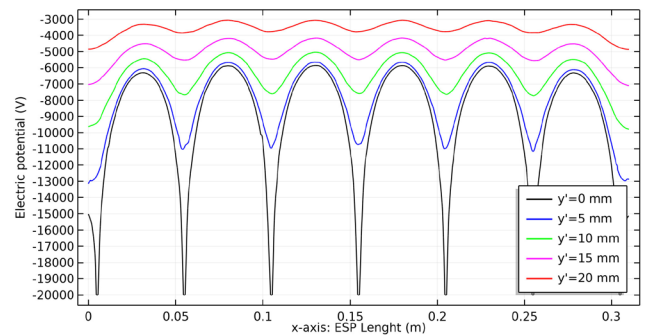


Fig. 6 Electric potential profiles to different distances from the corona wires.

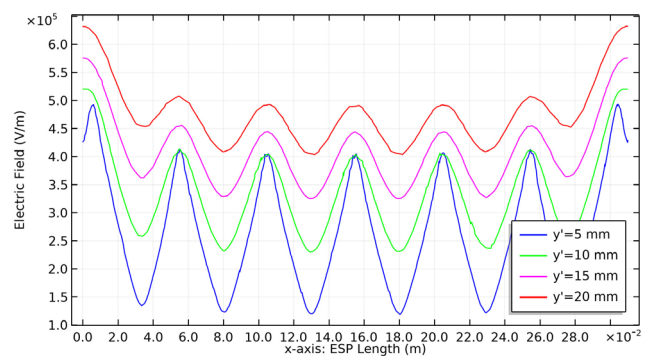


Fig. 7 Electric field (V/m) distribution along the corona wires.

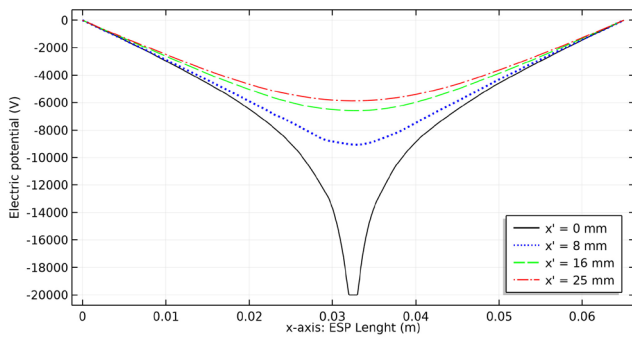


Fig. 8 Cutline between the collecting plates –20 (kV).

in Fig. 8. $x' = 0$ is placed at $x = 155$ mm, and when $x' = 25$ mm the cut line is equidistant between two corona wires.

The minimum potential values can be reached at $x'_{25\text{ mm}}$, and the maximum potential value is defined at $x' = 0$. The area between these two curves defines the electrical potential and its behavior from $x = 0$ to 310 mm. The same procedure is applied for the space charge density distribution, the results in magnitude are shown in Fig. 9. The maximum and minimum values are bounded in the corona wires axes and the half distance between the corona wires respectively.

5 Conclusions

Solving the PDEs along with the duct-type geometry allows the electrical phenomenon to be described, with the results obtained from simulation and some vertical or horizontal cuts inside the geometry allow understanding of how the electric potential, electric field, and space charge density change in magnitude within different sections of the ESP. The method used for solving the PDEs is not limited only to an ESP duct-type with seven corona wires.

References

[1] White, H. J. "Industrial Electrostatic Precipitation", Addison Wesley Publishing Company, Inc., Reading, MA, USA, 1963.
 [2] White, H. J. "Precipitator Design", Journal of the Air Pollution Control Association, 27(3), pp. 206–217, 1977.
<https://doi.org/10.1080/00022470.1977.10470412>
 [3] Gooch, J. P., Francis, N. L. "A Theoretically Based Mathematical Model for Calculation of Electrostatic Precipitator Performance", Journal of the Air Pollution Control Association, 25(2), pp. 108–113, 1975.
<https://doi.org/10.1080/00022470.1975.10470054>
 [4] Lawless, P. A. "Particle charging bounds, symmetry relations, and an analytic charging rate model for the continuum regime", Journal of Aerosol Science, 27(2), pp. 191–215, 1996.
[https://doi.org/10.1016/0021-8502\(95\)00541-2](https://doi.org/10.1016/0021-8502(95)00541-2)
 [5] Kiss, I., Iváncsy, T., Suda, J., Berta, I. "Modelling of Complex Physical Processes in Electrostatic Precipitators", Journal of Physics: Conference Series, 301, 012060, 2011.
<https://doi.org/10.1088/1742-6596/301/1/012060>

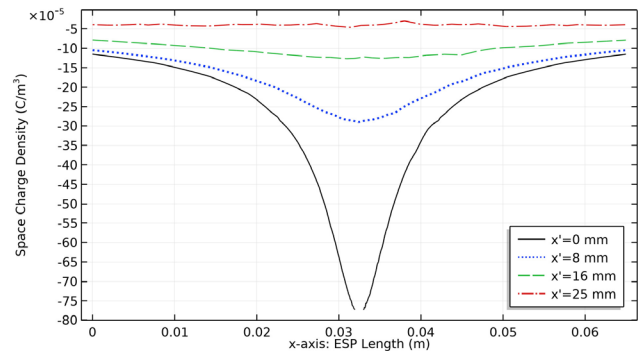


Fig. 9 Space charge density distribution (C/m³).

Therefore, it can be used for a different number of corona wires. Regarding the models for particle charging process, there are models more complex than others, based on the literature review the analysis between the theoretical and experimental data shows that they effectively describe the physical phenomena when the particles are being charged in different stages inside the ESP. For instance, Lawless' model has become more used in the new research because of its better results with particles of size about , where rarefactions occur.

Finally, the electrical phenomenon has been considered as an initial part of this work, and the found results allow us to proceed with the following topics to be discussed later, such as particle charging models, particle kinetics, and particle collection.

Acknowledgment

This work is supported by the Stipendium Hungaricum Scholarship.

[6] Kiss, I., Iváncsy, T., Berta, I. "Precipitation of Fine Particles Considering Uncertain Dust Properties", In: ICESP XI. International Society for Electrostatic Precipitation, Mpumalanga, South Africa, 2004, pp. 1–5.
 [7] White, H. J. "Particle Charging in Electrostatic Precipitation", Transactions of the American Institute of Electrical Engineers, 70(2), pp. 1186–1191, 1951.
<https://doi.org/10.1109/T-AIEE.1951.5060545>
 [8] Rubineti, D., Weiss, D., Egli, W. "Corona Discharge - A Fully Coupled Numerical Approach Verified and Validated", The International Journal of Multiphysics, 11(4), pp. 375–386, 2017.
<https://doi.org/10.21152/1750-9548.11.4.375>
 [9] Meroth, A. M., Gerber, T., Munz, C. D., Levin, P. L., Schwab, A. J. "Numerical solution of nonstationary charge coupled problems", Journal of Electrostatics, 45(3), pp. 177–198, 1999.
[https://doi.org/10.1016/S0304-3886\(98\)00046-1](https://doi.org/10.1016/S0304-3886(98)00046-1)

- [10] Adamiak, K., Atten, P. "Simulation of corona discharge in point–plane configuration", *Journal of Electrostatics*, 61(2), pp. 85–98, 2004.
<https://doi.org/10.1016/j.elstat.2004.01.021>
- [11] Potrymai, E., Perstnov, I. "Time Dependent Modelling and Simulation of the Corona Discharge in Electrostatic Precipitators", Master Thesis, Linnaeus University, 2014.
- [12] Lei, H., Wang, L. Z., Wu, Z. N. "EHD turbulent flow and Monte-Carlo simulation for particle charging and tracing in a wire-plate electrostatic precipitator", *Journal of Electrostatics*, 66(3–4), pp. 130–141, 2008.
<https://doi.org/10.1016/j.elstat.2007.11.001>
- [13] Zhao L, Adamiak K. "Electrohydrodynamic flow produced by electric corona discharge (numerical and experimental studies, and applications)", In: 2009 Electrostatics Joint Conference, Boston, MA, USA, 16–18. June, 2009.
- [14] Lancereau, Q., Roux, J. M., Achard, J. L. "Electrohydrodynamic flow regimes in a cylindrical electrostatic precipitator", *IEEE Transactions on Dielectrics and Electrical Insulation*, 20(4), pp. 1409–1420, 2013.
<https://doi.org/10.1109/TDEI.2013.6571463>
- [15] Ruttanachot, C., Tirawanichakul, Y., Tekasakul, P. "Application of Electrostatic Precipitator in Collection of Smoke Aerosol Particles from Wood Combustion", *Aerosol and Air Quality Research*, 11(1), pp. 90–98, 2011.
<https://doi.org/10.4209/aaqr.2010.08.0068>
- [16] Pal, A., Dixit, A., Srivastava, A. K. "Design and optimization of the shape of electrostatic precipitator system", *Materials Today: Proceedings*, 47(13), pp. 3871–3876, 2021.
<https://doi.org/10.1016/j.matpr.2021.03.448>
- [17] Wang, Y., Zhang, H., Gao, W., Shao, L., Wu, Z., Zhao, Z., Ge, C., Hu, D., Zheng, C., Gao, X. "Improving the removal of particles via electrostatic precipitator by optimizing the corona wire arrangement", *Powder Technology*, 388, pp. 201–211, 2021.
<https://doi.org/10.1016/j.powtec.2021.04.087>
- [18] Shen, H., Yu, W., Jia, H., Kang, Y. "Electrohydrodynamic flows in electrostatic precipitator of five shaped collecting electrodes", *Journal of Electrostatics*, 95, pp. 61–70, 2018.
<https://doi.org/10.1016/j.elstat.2018.08.002>
- [19] Liu, L. "Physics of Electrical Discharge Transitions in Air", Doctoral thesis, KTH Royal Institute of Technology, 2017.
- [20] Li, S., Huang, Y., Zheng, Q., Deng, G., Yan, K. "A numerical model for predicting particle collection efficiency of electrostatic precipitators", *Powder Technology*, 347, pp. 170–178, 2019.
<https://doi.org/10.1016/j.powtec.2019.02.040>
- [21] Zhu, J., Zhao, Q., Yao, S., Guo, X., Zhang, X., Zeng, Y., Yan, K. "Effects of high-voltage power sources on fine particle collection efficiency with an industrial electrostatic precipitator", *Journal of Electrostatics*, 70(3), pp. 285–291, 2012.
<https://doi.org/10.1016/j.elstat.2012.03.009>
- [22] Haque, S. M. E., Rasul, M. G., Khan, M. M. K. "Modelling and Simulation of an Electrostatic Precipitator", In: Murphy, A. D. (ed.) *Computational Fluid Dynamics: Theory, Analysis and Applications*, pp. 267–296, NOVA Science Publishers, Inc., 2010. ISBN 1612092764
- [23] Bäck, A., Cramsky, J. "Comparison of Numerical and Experimental Results for the Duct-Type Electrostatic Precipitator", *International Journal of Plasma Environmental Science & Technology*, 6(1), pp. 33–42, 2012.
- [24] Rubinetti, D., Weiss, D. A., Egli, W. "Electrostatic Precipitators-Modelling and Analytical Verification Concept", In: COMSOL Conference 2015, Grenoble, France, 14–16. Oct., 2015. [online] Available at: https://www.comsol.com/paper/download/291561/rubinetti_paper.pdf [Accessed: 03 November 2021]
- [25] Iváncsy, T., Suda, J. M. "Behavior of polydisperse dust in electrostatic precipitators", *Journal of Electrostatics*, 63(6–10), pp. 923–927, 2005.
<https://doi.org/10.1016/j.elstat.2005.03.062>
- [26] Diga, S. M., Sirbu, I. G., Diga, N. "Computer aided dimensioning of the electrostatic precipitators for energy blocks", In: 2013 8th International Symposium on Advanced Topics in Electrical Engineering (ATEE), Bucharest, Romania, 2013, pp. 1–6. ISBN: 978-1-4673-5979-5
<https://doi.org/10.1109/ATEE.2013.6563519>
- [27] Buccella, C. "Computation of V - I characteristics in electrostatic precipitators", *Journal of Electrostatics*, 37(4), pp. 277–291, 1996.
[https://doi.org/10.1016/0304-3886\(96\)00022-8](https://doi.org/10.1016/0304-3886(96)00022-8)
- [28] Dong, M., Zhou, F., Zhang, Y., Shang, Y., Li, S. "Numerical study on fine-particle charging and transport behaviour in electrostatic precipitators", *Powder Technology*, 330, pp. 210–218, 2018.
<https://doi.org/10.1016/j.powtec.2018.02.038>
- [29] Gao, W., Wang, Y., Zhang, H., Guo, B., Zheng, C., Guo, J., Gao, X., Yu, A. "Numerical simulation of particle migration in electrostatic precipitator with different electrode configurations", *Powder Technology*, 361, pp. 238–247, 2020.
<https://doi.org/10.1016/j.powtec.2019.08.046>
- [30] Arif, S., Branken, D. J., Everson, R. C., Neomagus, H. W. J. P., le Grange, L. A., Arif, A. "CFD modeling of particle charging and collection in electrostatic precipitators", *Journal of Electrostatics*, 84, pp. 10–22, 2016.
<https://doi.org/10.1016/j.elstat.2016.08.008>
- [31] Zhu, Y., Gao, M., Chen, M., Shi, J., Shangguan, W. "Numerical simulation of capture process of fine particles in electrostatic precipitators under consideration of electrohydrodynamics flow", *Powder Technology*, 354, pp. 653–675, 2019.
<https://doi.org/10.1016/j.powtec.2019.06.038>